Seismic Sloshing Effects in Lead-Cooled Fast Reactors

M. Jeltsov, W. Villanueva, P. Kudinov

KTH Royal Institute of Technology, Stockholm, Sweden

E-mail contact of main author: marti@safety.sci.kth.se

Abstract. Pool-type primary system of an LFR (lead-cooled fast reactor) allows for simple and economic reactor design. However, filling this pool partially with heavy liquid metal poses safety concerns due to seismicity. Violent sloshing during earthquake-initiated FSI (fluid-structure interaction) can lead to structural failures, gas entrapment and potential core voiding. Seismic isolation systems can be used to reduce the structural stresses, but its effect on sloshing requires separate evaluation.

A CFD (computational fluid dynamics) study of sloshing in ELSY reactor has been carried out. Analyzed cases include a fixed base reactor case and seismically isolated reactor cases are modelled using synthetic earthquake data produced in SILER project. Free surface motion is modelled with a VOF (volume of fluid) method. Verification and validation of the numerical model is presented.

The adverse effect of seismic isolation system in terms of sloshing-induced hydrodynamic loads and gas entrapment are demonstrated. Furthermore, effects of geometry on sloshing have been discussed. A mitigation solution using flow restrictions has been proposed and analyzed.

Key Words: LFR, CFD, Seismic Sloshing, FSI, Gas Entrapment.

1. Introduction

Lead-cooled fast reactor (LFR) is identified as one of the six most promising Generation IV reactor designs [1], [2]. A number of LFR designs are currently being developed worldwide [3]. Majority of those feature a pool-type primary system that accommodates most of the important reactor components, i.e. core, pumps, steam generators (SGs) and lead coolant. Such design solution represents essentially an elevated pool filled partially with high density liquid which poses concerns regarding seismicity. A comprehensive overview of earthquake related problems in nuclear reactors can be found in [4]–[7]. Of many potential issues described there, sloshing of heavy coolant has to be carefully accounted for in the design and safety analysis of LFR primary systems [8]. Decision-making process in a *high-consequence* field such as nuclear safety requires adequate computational tools whose prediction credibility is of paramount importance since the effects of the success or failure of the project have major consequences beyond the project itself [9]. The latter makes the verification and validation of the models used very important.

Sloshing means any motion of the free liquid surface in its container [10]. Sloshing can be caused by internal (e.g. vortices, chemical reactions) or external disturbances (e.g. seismic events, motion of tanker ships and trucks). Increased mechanical loads during sloshing-induced fluid-structure interaction (FSI) can lead to structural failures, i.e. plastic deformation when exceeding the yield stress and rupture when exceeding the ultimate tensile strength. In LFRs, this phenomenon is particularly critical in the upper part of the primary vessel where lead-argon interface intersects with several reactor components (e.g. SGs, core barrel, fuel and control rods). Moreover, the reactor roof can be subject to high pressure impacts due to waves moving

upwards at the vertical walls. The SL-1 reactor accident in US is an example to illustrate forces created by moving liquid. A sudden enormous power excursion caused water to accelerate 0.76 m upwards and struck the vessel head at 49 m/s with a pressure of 690 bar causing the 12,000 kg steel vessel to jump 2.77 m before it dropped into its prior location [11]. Another potential consequence of violent sloshing, in addition to mechanical damage, is the gas entrapment due to strongly deformed and disintegrated liquid-gas interface. Subsequent entrainment of gas to the core region can lead to (i) reactivity initiated accident (RIA) due to locally positive void reactivity coefficients in LFRs, or (ii) local dry-out of the fuel rods [12].

One of the mitigation strategies for earthquake-induced events is to use seismic isolation systems. This system consists of a set of seismic isolator devices under a superstructure (e.g. nuclear reactor building) with the aim to reduce the stresses in the superstructure by reducing the fundamental frequencies in the response spectrum at the point of interest compared to the ground motion. This frequency shift however, brings the system closer to liquid sloshing frequencies as demonstrated in a parametric sloshing study by Jeltsov et al. [13].

The goal of this paper is to study the effect of seismic excitation and isolation system on liquid lead sloshing in ELSY primary system.

2. Overview of sloshing modeling approaches

Early approaches used to study sloshing phenomenon, including mass-spring and tank-liquid analogies, are well described in works of Housner and his colleagues [4], [6], [7]. Development of finite elements based computational fluid dynamics (CFD) methods for FSI problems with special attention to the non-linear free surface motion and the tank buckling dates back to early 1980's. One of the first numerical tools for FSI problems is a computer code FLUSTR that uses Arbitrary Eulerian-Lagrangian (ALE) formulation to model fluid flow and solid behavior simultaneously [8], [14], [15]. ALE is an adequate approach for separate treatment of and interaction between fluid and structural domains. ALE approach was used to study the structural response and lead sloshing during a safe shutdown earthquake of the ELSY reactor [16]. It was demonstrated that the presence of internal components reduces sloshing.

Another method used to analyze sloshing problems is meshless Smooth Particle Hydrodynamics (SPH). SPH analysis of a dam break and centralized liquid sloshing experiments have shown that the method predicts the general flow fields reasonably well but requires special attention to accurately model the viscosity and wall effects [17].

With further developments in the CFD arena, the volume of fluid (VOF) method developed by Hirt and Nichols [18] has been used in many recent sloshing studies. As a fixed-grid method, VOF is very efficient for flows where the phases are largely separated and the interfacial area is relatively small. The main strengths of the VOF method are the enforcement of mass conservation and the ability to track steep and highly contorted free surface (see examples in [19]–[24]).

3. ELSY reactor

ELSY is a conceptual pool-type LFR designed for efficient and safe power production fully compliant with the Generation IV goals for sustainability, safety and reliability, economic competitiveness and proliferation resistance and physical protection [25]–[27]. ELSY produces 1500 MW of thermal power that is transferred to the secondary cycle through eight SGs. The system contains about 6000 tons of liquid lead out of approximately 8000 tons of total mass of the primary system. There is a gas plenum filled with argon above the lead pool to accommodate coolant thermal expansion and temperature gradient between hot lead and the reactor roof. The

primary system configuration is shown in FIG. 1. The relatively short height of ELSY reactor (<10 m) is an advantage in terms of seismic performance. Yet, many internals "hanging" from the roof, heavy structures and components in the reactor building still call for a seismic isolation system to achieve highest levels of safety. Regarding gas entrainment, the spectral effect of coolant voiding in the core region of an LFR (where neutron leakage has a small effect) is generally positive due to reduced neutron moderation and capture (i.e., the spectrum becomes harder due to voiding) [28].

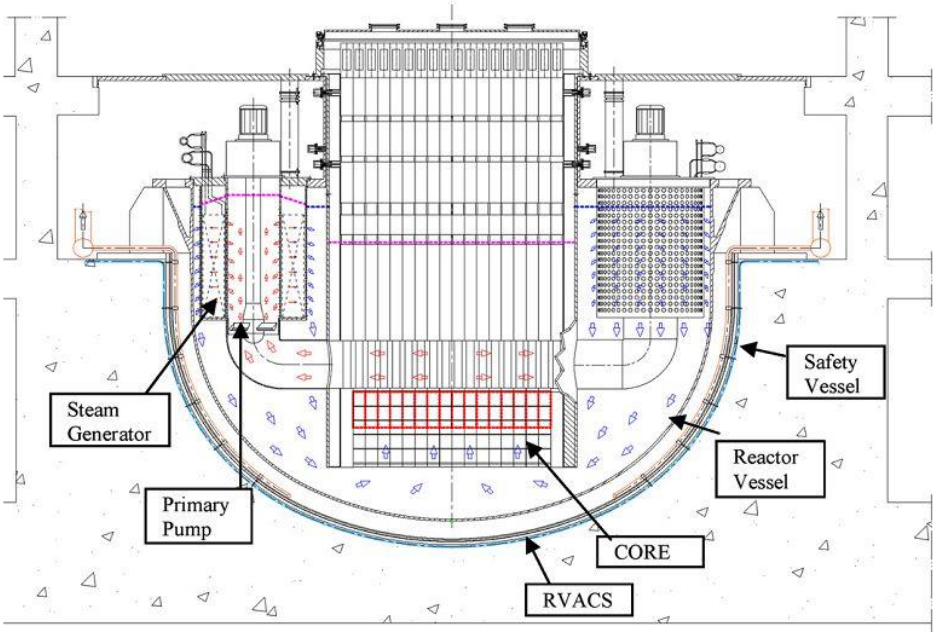

FIG. 1. ELSY primary system configuration [25].

4. Seismic input

Synthetic earthquake data produced in SILER project [29] was used as an input in this study. The data consists of time-histories and corresponding spectra of accelerations, velocities and displacements calculated at a point (IP1B) on the supporting ring of the vessel (FIG. 2). This is the spectra that the liquid in the pool is assumed to be subject to. Two seismic cases have been studied: Case 1 representing a fixed-base reactor under a Design Basis Earthquake (DBE) and Case 2 representing a seismically-isolated reactor using Lead Rubber Bearings (LRB) (see FIG. 3) subject to Beyond DBE (BDBE) level earthquake. See details in TABLE I.

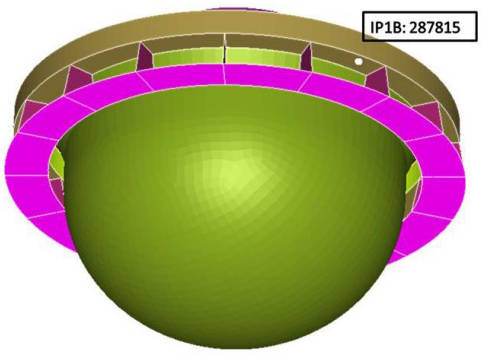

FIG. 2: Location of the interface point IP1B on the reactor vessel supporting ring.

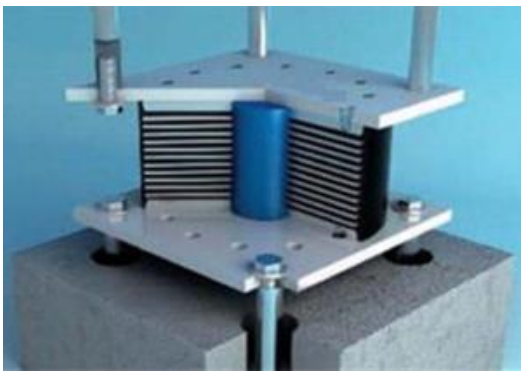

FIG. 3: Lead Rubber Bearing (LRB). An elastomeric isolation device with lead core.

TABLE I: SEISMIC CASES.

Case	Seismic level	Isolator type	Soil type
1	DBE: - peak ground acceleration 0.3 g - peak ground displacement 22 cm	N/A	Hard (NRC RG 1.60 for Central and Eastern US [30])
2	BDBE: - peak ground acceleration 0.9 g - peak ground displacement 70 cm	LRB	

The accelerograms and response spectra (calculated with Fast Fourier Transform) are show in FIG. 4 and FIG. 5 for the DBE and BDBE cases, respectively. In case of DBE with no IS, the horizontal accelerations of up to 2 g at 5 Hz are detected. Even though the BDBE is associated with a stronger ground acceleration, the use of LRB IS leads to 2 times lower horizontal loads compared to DBE with no IS. The frequencies are shifted from 5 Hz to 0.5 Hz, i.e. closer to natural frequencies of liquid sloshing in LFRs [13]. Amplification of the vertical response is a common feature of LRBs observed both numerically and experimentally [31], [32]. This, however, is not a concern since the structures are designed to withstand vertical loads and the gravity provides sufficient damping of free surface motion in vertical direction.

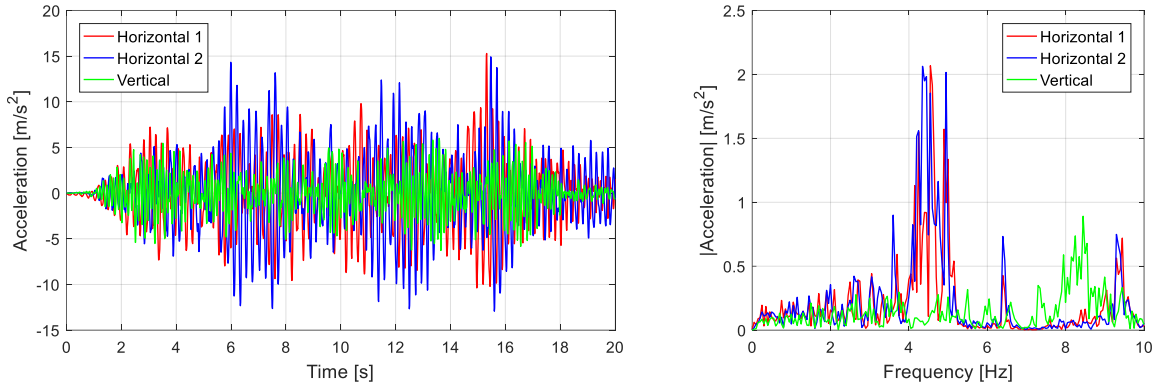

FIG. 4. Acceleration time-histories and spectra of Case 1.

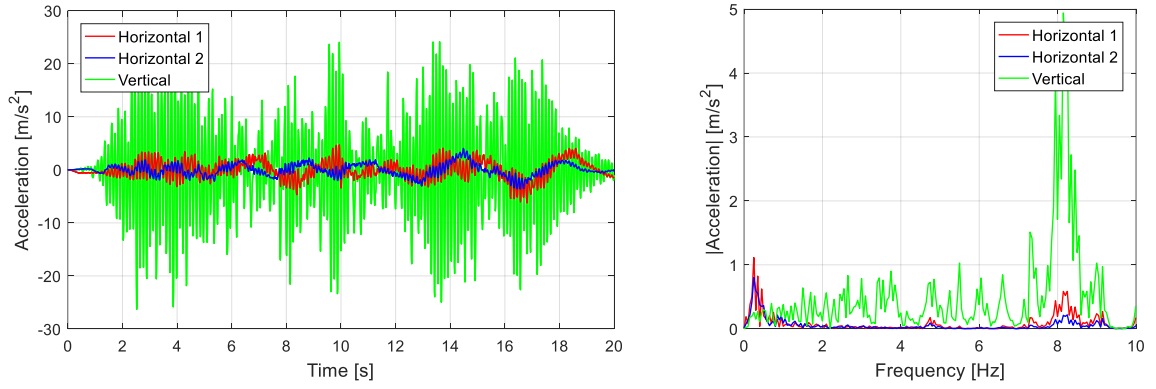

FIG. 5. Acceleration time-histories and spectra of Case 2.

5. CFD model

Modeling of sloshing, a multi-phase problem, requires adequate descriptions for the liquid and gas phases as well as the interaction between them in order to determine the location of the interface, i.e. the free surface.

In this work, a commercial software Star-CCM+ v. 11.02.009 was used [33]. The CFD model includes only fluid domain meaning that all reactor structures are assumed rigid. Fluid flow fields have been modeled with a Reynolds-Averaged Navier-Stokes (RANS) approach using two-equation Realizable k-epsilon linear eddy viscosity model for turbulence. All-y^+ wall treatment has been used to effectively account for the wide range of spatial and temporal velocity variations in the domain during seismic event. The free-surface has been modeled with VOF interface capturing method [18]. VOF is a homogeneous Eulerian multiphase model where a common velocity, temperature and pressure field is assumed for all phases. The sharp interface is reconstructed using a High-Resolution Interface Capturing (HRIC) scheme [33]. Constant properties at 440 °C have been used for liquid lead [34] while argon has been modelled as ideal gas. Surface tension is calculated as a function of the fluid-gas properties, temperature and the surface curvature. Segregated solvers are used for velocity, pressure, volume fraction and turbulent properties. The under-relaxation factors are 0.8 for velocity, 0.2 for pressure, 0.9 for volume fraction and energy, 0.8 for turbulent kinetic energy and 1.0 for turbulent dissipation rate. 10 iterations per time-step were used.

5.1.Verification and validation

Since there is no experimental data available for lead sloshing or ELSY reactor, it is imperative to assure that the model represents the relevant phenomena and the solution is verified. Numerical spatial and temporal discretization of the governing equations plays an important role in the accurate prediction of free-surface motion and related hydrodynamic forces during violent sloshing (e.g. breaking waves, dispersion of one phase into another, formation of bubbles and droplets). Mesh and time-step size selection is studied and discussed below.

Time-step

Sloshing is a transient phenomenon. Selection of time-step size for unsteady calculations must take into account the characteristics of the unsteady boundary conditions (physical criterion) and model requirements (numerical criterion). While important, satisfying these criteria may not be sufficient for the convergence of the finite-difference approximation of the numerical problem. Thus, an independence study of refining the step-size until the solution does not change any more shall be used.

Physical criterion in this work is defined by the seismic acceleration spectra which contains frequencies up to 10 Hz. Desired resolution of 100 increments per period results in time-step of 1 ms. Numerical criterion comes from the CFL condition in the HRIC scheme used in the VOF model that is optimized for Courant number 0.5 to avoid excessive diffusion of the interface. Assuming characteristic velocity of 10 m/s and 5 cm cell size leads to time-step of 2.5 ms. Automatic time-step calculation was implemented in Star-CCM+ as:

$$\Delta t^n = \frac{Co_{target}}{Co_{max}} \Delta t^{n-1} \quad (1)$$

Keeping the Courant number constant ensures automatically the optimum time-step size for a given mesh.

Mesh

Mesh study was carried out using the dam break experiment conducted at the Maritime Research Institute Netherlands [35]. In the test, a box of 16 cm × 40 cm × 16 cm was placed in a 3.2 m × 1 m × 1 m tank with an open roof. Initially, 0.55 m high water column was held by a vertical wall at a distance of $x = 2\ m$. Water was released after sudden lifting of the wall by releasing a weight.

Since it is regarded adequate to approximate this dam break experiment to a 2D flow and considering the need for large number of calculations, a 2D model was used for the mesh study. It can be argued that the requirements sloshing phenomenon sets on the numerical discretization in 2D are valid also in 3D. The initial state is shown in FIG. 6. Automatic time-stepping with $Co_{target} = 0.5$ was used. All spatial and temporal discretization schemes used were of 2nd order. All meshes used polyhedral elements.

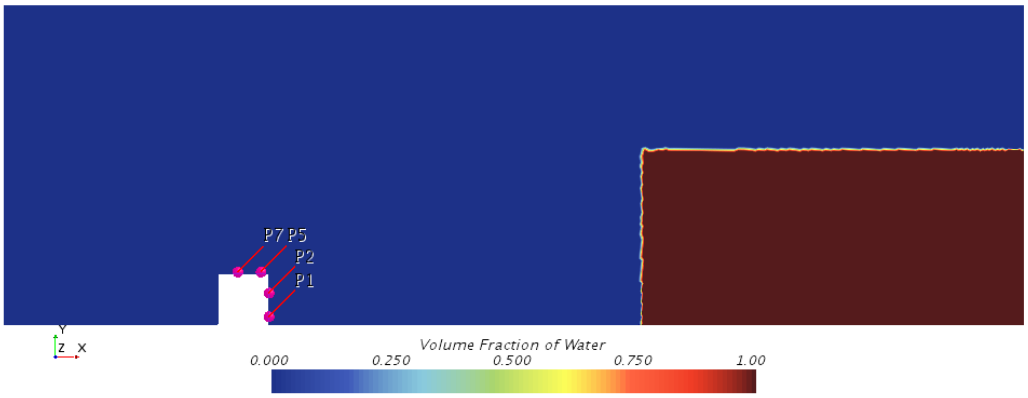

FIG. 6. Initial state of the 2D dam break model and pressure monitor locations on the box (P1-P7).

FIG. 7 shows that pressure variation at P1 with two peaks around 0.4 s and 4.6 is captured reasonably well all meshes. A small but consistent delay of ~20 ms in the first peak prediction can be attributed to uncertainty in the initial conditions i.e. size and location of the initial water column; timing and simultaneity of release (jet formation, upward shear when lifting the wall); water properties; and/or geometric fidelity. Subsequent over-prediction of the peak pressure values (~15-18 kPa versus ~11 kPa in exp.), is potentially directly related to that delay. The numerical oscillations at about 1.3 s when the water returns from the left wall and overturns the box were observed here and also in [35].

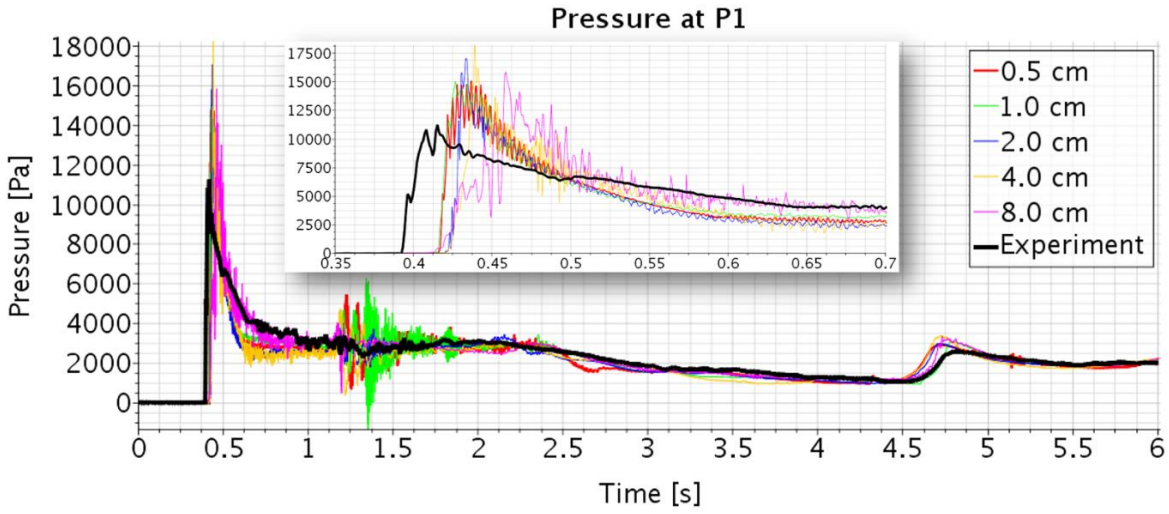

FIG. 7. Pressure at sensor P1 with different mesh sizes.

This study shows that, if the CFL criterion is respected, the mesh size has a relatively small effect. Consequently, cell size of 2.5 cm was selected for the 3D analysis based on the following aspects: acceptable computation time, sufficient resolution of large-scale sloshing flow and acceptable accuracy in impact pressure prediction. It is acknowledged that using this mesh the fine dispersion (scales < 2.5 cm) of gas cannot be resolved. However, as we are interested in tendencies of void formation (possibility of gas entrapment and the size/location/velocity of the gas in the coolant) and not actual sizes of bubbles, it is an acceptable sacrifice.

6. Sloshing in ELSY reactor

6.1. Model description

The 3D analysis focuses on region between two neighboring SGs (FIG. 8). Mesh of ~750,000 polyhedral elements is created automatically. Physics models remain the same as in the 2D study, except that the three-dimensional seismic excitation is applied through a time-dependent momentum source. Symmetry conditions are applied to section side boundaries. The flow is assumed initially to be at rest with the liquid level flat at nominal condition. Duration of the earthquake is 20 s.

The quantities of interest monitored in this study include maximum pressures at all solid structures, wave height, gas submersion depth and the amount of gas reaching at 1 m below the initial free surface location is of interest.

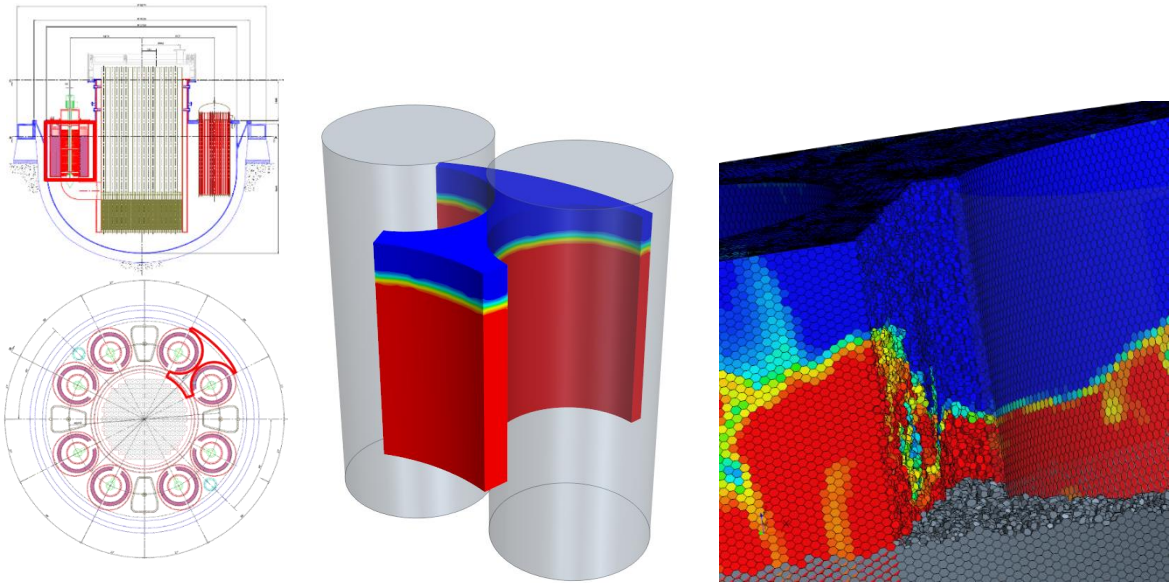

FIG. 8. 3D domain definition, initial solution (red-Pb, blue-Ar) and a mesh of 750,000 poly elements.

CFD simulations revealed that the flow congestion and acceleration in the narrow gap between the SGs (i) exerts lateral forces (with respect to the flow direction in the gap) on SGs and (ii) gives rise to slamming due to forces normal to the inner and outer vessels (see FIG. 9). Since the seismic excitation is asymmetric by nature, an imbalance of forces on either side of an SG can result in displacements that create stresses in the pipes that connect SGs to the core barrel.

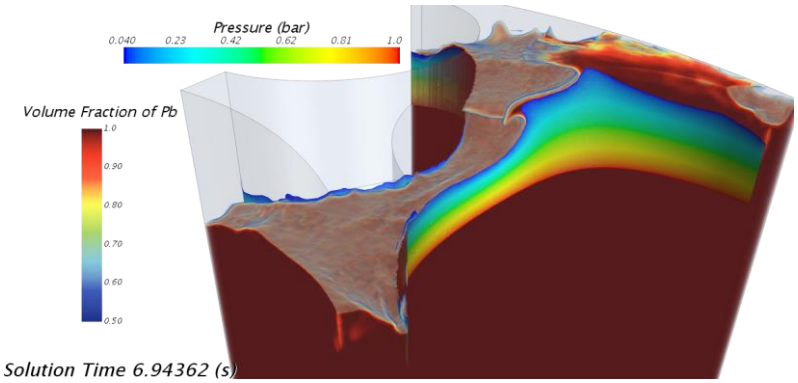

FIG. 9:Flow congestion and acceleration between SGs.

6.2.Effect of seismic isolation system

In order to demonstrate the effect of IS, the results of Case 1 (no IS) and Case 2 (LRB isolated) are compared. Maximum pressures monitored on solid walls of the primary system are shown in FIG. 10. One of the most critical surfaces with respect to dynamic loading is the bolted reactor roof since it supports most of the reactor internals.

In Case 1, the vertical reactor walls experience only impulsive pressures, i.e. those associated with the inertial forces directly proportional to the seismic excitation and fluid weight. Reactor roof and SG walls experience some slamming (up to 35 bar) due to convective pressures, i.e. the forces produced by the impact of sloshing waves on a surface.

In Case 2, the pressure spikes of up to 1500 bar on the vessel and core barrel are observed while reactor roof experiences slamming at about 700 bar. This demonstrates the adverse effect of the spectral frequency shift due to seismic isolation system.

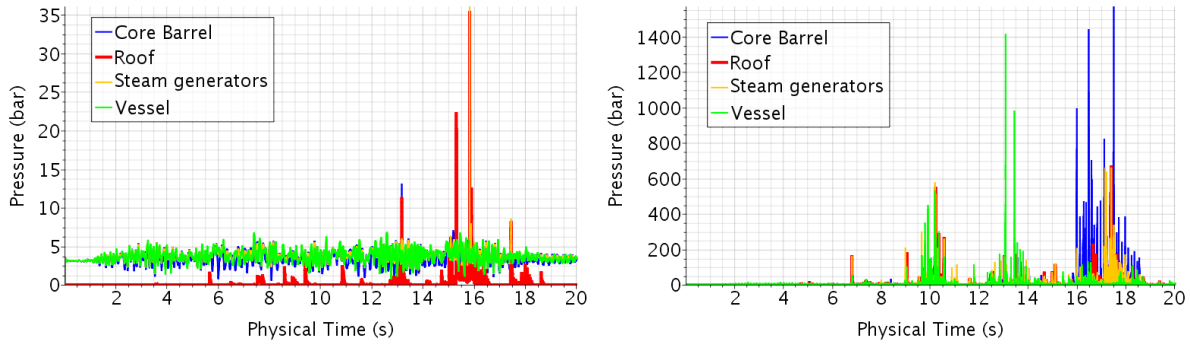

FIG. 10: Pressure maxima on solid walls (fixed-base reactor – left, seismically isolated reactor - right).

Wave height and gas submersion depth are shown in FIG. 11. In fixed-base reactor, gas reaches 0.8 m below initial free surface, while in seismically isolated reactor gas is detected at depths more than 2 m. Up to hundreds of liters of gas are found deeper than 1 m below free surface (FIG. 12).

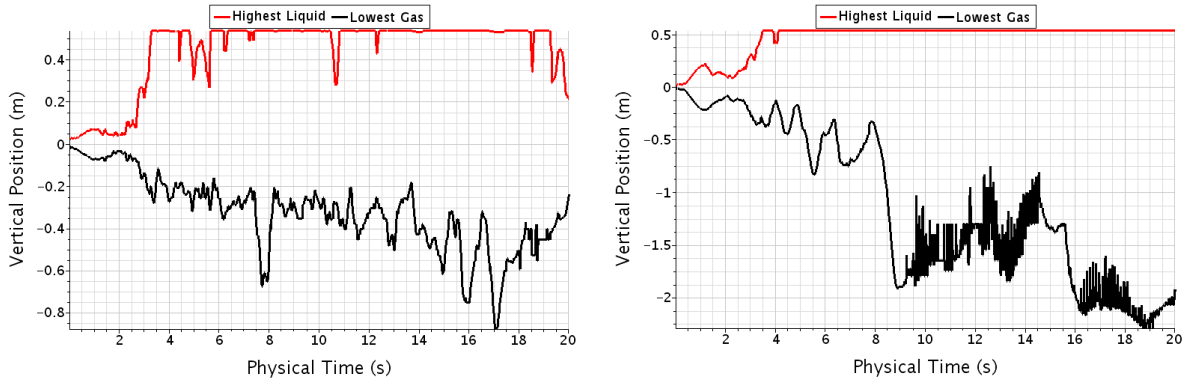

FIG. 11: Maximum liquid height and gas submersion depth (fixed-base reactor – left, seismically isolated reactor - right).

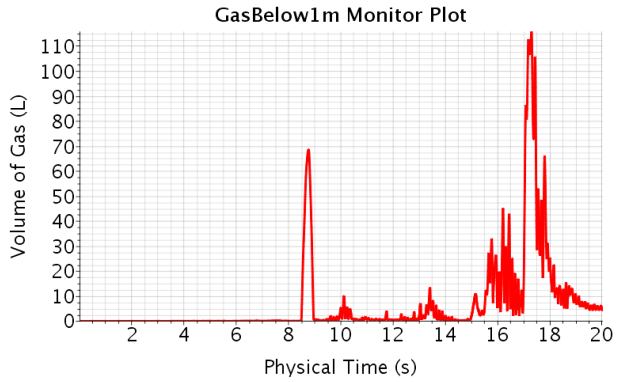

FIG. 12: Amount of gas below 1 m in Case 2.

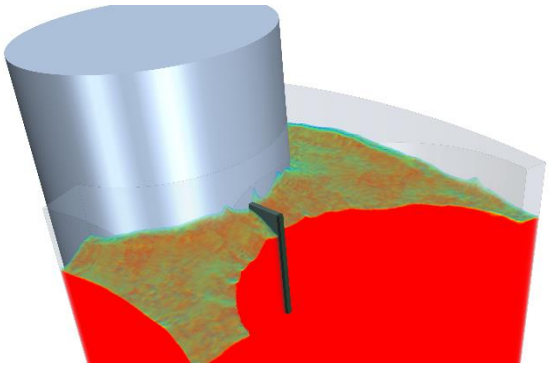

FIG. 13: A thin baffle between two SGs.

6.3.Effect of internal baffle

Due to high dynamic loading of structures during violent sloshing in Case 2, a mitigation solution is proposed in the form of a flow obstructing baffle intersecting the free surface between two SGs (dark grey slab in FIG. 13). Partitioning space using baffles in the flow effectively decreases the characteristic length scales leaving the fluid with less space/time to accelerate resulting in smaller convective forces – a common practice in LNG cargo tanks, for example. Moreover, the sharp-edged baffle enhances the production of turbulence and its subsequent dissipation when the fluid splashes on the free surface at the other side of the baffle. The baffle implemented here is 5 cm thick and extends 0.1 m above and 1.0 m below the free surface. Note that the dimensions are tentative as the specific design is of no interest here.

Pressure maxima using baffle is shown in FIG. 14. In Case 1 (fixed-base, DBE), the roof pressure is reduced from 35 bar to virtually zero, i.e. slosh waves do not reach the roof. In Case 2 (LRB IS, BDBE), the use of baffle reduces sloshing/slamming pressures on the roof from 700 to 230 bar. This reduction comes at a cost though – the baffle itself bears loads (up to ~750 bar) that has to be accounted for in its actual design (e.g. fixing the baffle to an SG, using a flexible flap from the roof). Loads on the SG walls and core barrel remain very high despite the baffle.

In Case 1, the baffle also reduces the wave heights and gas submersion (FIG. 15, left). However, in Case 2, the gas entrapment is not significantly affected (FIG. 15, right). FIG. 16 illustrates the process of wave breaking over the baffle and engulfment of a gas bubble.

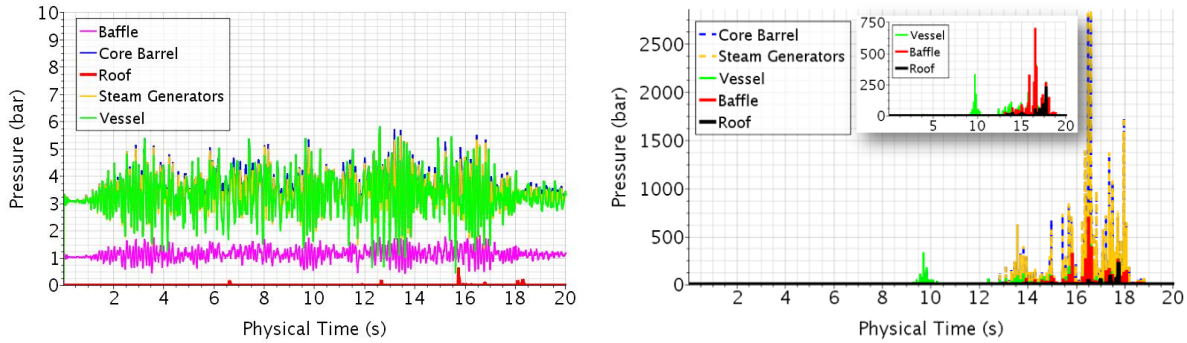

FIG. 14: Pressure maxima on solid walls with baffle
(fixed-base reactor – left, seismically isolated reactor - right).

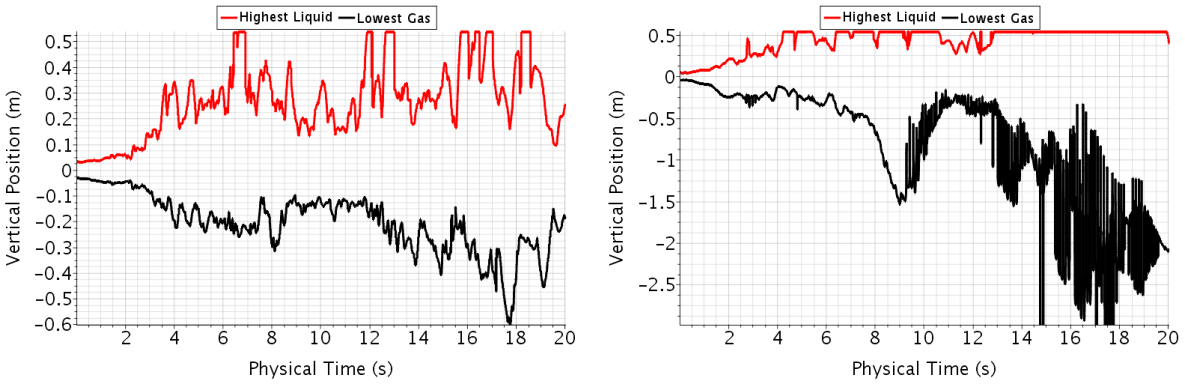

FIG. 15: Maximum liquid height and gas submersion depth with baffle (fixed-base reactor – left, seismically isolated reactor - right).

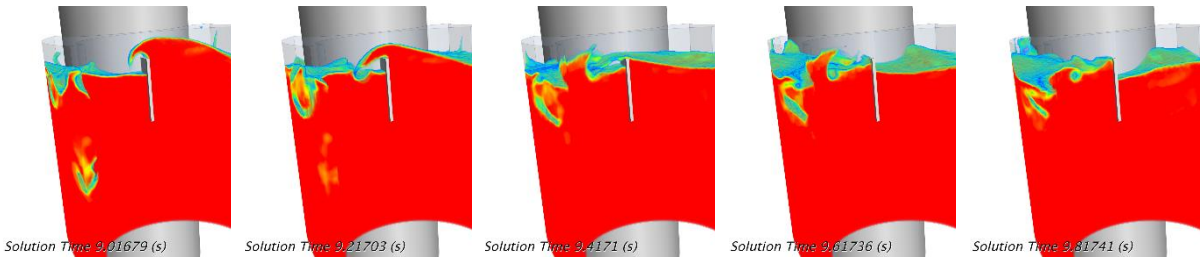

FIG. 16: Snapshots of wave overturning and splashing into the fluid on the other side of the baffle.

7. Summary and conclusions

This paper presents a CFD study of seismic sloshing phenomena in LFRs. This multiphase problem has been simulated using a Eulerian RANS solver coupled with VOF model to capture the gas-liquid interface in a computationally efficient manner. A dam break experiment was used in a combined solution verification/validation exercise which showed that it is important to satisfy the requirements on Courant number set by the VOF interface reconstruction scheme.

3D analysis of sloshing in the inter-SG region of ELSY reactor was performed for fixed based and seismically isolated reactor cases at different earthquake levels. It was found that the flow congestion in the gap between SGs pronounces the normal and lateral loads on the core barrel/reactor vessel and SG walls, respectively. Moreover, the effect of seismic IS on sloshing response in terms of sloshing pressures has been demonstrated.

A mitigation solution consisting of a simple baffle implemented in the free surface region between the SGs has been proposed. A positive effect of such solution in reducing the loads on important reactor components (e.g. roof, SGs) is demonstrated in both, fixed base and seismically isolated cases. A specific design of the obstructing baffle is crucial since it experiences high loads itself. As the baffle reduces the characteristic length scales in the domain, an equivalent effect could be achieved by reducing the gas plenum height.

The assumption of rigidity used for all structures should be assessed by performing local mechanical and/or FSI analysis taking into account sloshing loads. In critical regions, it is important to take the realistic operating conditions (e.g. temperature) into account. Also, full 3D analysis of LFRs is of interest due to the asymmetric nature of seismic excitation.

8. Acknowledgements

This study has been supported by the EU-FP7-EURATOM-FISSION project SILER (project reference 295485). The 3D simulations were performed on resources provided by the Swedish

National Infrastructure for Computing (SNIC) at PDC Centre for High Performance Computing (PDC-HPC).

References

[1] U.S. DOE Nuclear Energy Research Advisory Committee and The Generation IV International Forum, "A Technology Roadmap for Generation IV Nuclear Energy Systems," GIF-002-00, Dec. 2002.

[2] GEN IV International Forum, "GIF R&D Outlook for Generation IV Nuclear Energy Systems," 2009.

[3] A. Alemberti, "The Lead Fast Reactor: An Opportunity for the Future?," *Engineering*, vol. 2, no. 1, pp. 59–62, Mar. 2016.

[4] G. W. Housner and D. E. Hudson, "Earthquake research problems of nuclear power plants," *Nucl. Eng. Des.*, vol. 3, pp. 308–319, 1966.

[5] J. D. Stevenson, R. P. Kennedy, and W. J. Hall, "Nuclear power plant seismic design—A review of selected topics," *Nucl. Eng. Des.*, vol. 79, no. 1, pp. 7–18, May 1984.

[6] G. W. Housner, "Dynamic pressures on accelerated fluid containers," *Bull. Seismol. Soc. Am.*, vol. 47, no. 1, pp. 15–35, 1957.

[7] G. W. Housner, "The Dynamic Behavior of Water Tanks," *Bull. Seismol. Soc. Am.*, vol. 53, no. 2, pp. 381–387, 1963.

[8] D. C. Ma, W. K. Liu, J. Gvildys, and Y. W. Chang, "Seismically-Induced Sloshing Phenomena in LMFBR Reactor Tanks," Argonne, IL, 1982.

[9] W. L. Oberkampf and C. J. Roy, *Verification and validation in scientific computing*. Cambridge University Press, 2010.

[10] R. A. Ibrahim, *Liquid sloshing dynamics: theory and applications*. Cambridge University Press, 2005.

[11] J. F. Kunze, "Additional Analysis of the SL-1 Excursion, Final Report of Progress, July through October 1962." IDO-19313, US Department of Energy, Idaho Operations Office, Idaho Falls, Idaho, 1962.

[12] M. Jeltsov and P. Kudinov, "Simulation of a steam bubble transport in the primary system of the pool type lead cooled fast reactors," in *14th International Topical Meeting on Nuclear Reactor Thermalhydraulics (NURETH-14)*, 2011.

[13] M. Jeltsov, W. Villanueva, and P. Kudinov, "Parametric Study of Sloshing Effects in the Primary System of an Isolated Lead-Cooled Fast Reactor," *Nucl. Technol.*, vol. 190, no. 1, pp. 1–10, 2015.

[14] W. K. Liu, "Finite element procedures for fluid-structure interactions and application to liquid storage tanks," *Nucl. Eng. Des.*, vol. 65, no. 2, pp. 221–238, 1981.

[15] W. K. Liu and D. C. Ma, "Computer implementation aspects for fluid-structure interaction problems," *Comput. Methods Appl. Mech. Eng.*, vol. 31, no. 2, pp. 129–148, Jul. 1982.

[16] R. Lo Frano and G. Forasassi, "Preliminary evaluation of the seismic response of the ELSY LFR," *Nucl. Eng. Des.*, vol. 242, pp. 361–368, Jan. 2012.

[17] A. Vorobyev, V. Kriventsev, and W. Maschek, "Simulation of central sloshing experiments with smoothed particle hydrodynamics (SPH) method," *Nucl. Eng. Des.*,

vol. 241, no. 8, pp. 3086–3096, Aug. 2011.

[18] C. . Hirt and B. . Nichols, “Volume of fluid (VOF) method for the dynamics of free boundaries,” *J. Comput. Phys.*, vol. 39, pp. 201–225, 1981.

[19] M. S. Celebi and H. Akyildiz, “Nonlinear modeling of liquid sloshing in a moving rectangular tank,” *Ocean Eng.*, vol. 29, no. 12, pp. 1527–1553, Sep. 2002.

[20] P. C. Sames, D. Marcouly, and T. E. Schellin, “Sloshing in rectangular and cylindrical tanks,” *J. Sh. Res.*, vol. 46, no. 3, pp. 186–200, 2002.

[21] M. Eswaran, U. K. Saha, and D. Maity, “Effect of baffles on a partially filled cubic tank: Numerical simulation and experimental validation,” *Comput. Struct.*, vol. 87, no. 3–4, pp. 198–205, Feb. 2009.

[22] P. Ming and W. Duan, “Numerical simulation of sloshing in rectangular tank with VOF based on unstructured grids,” *J. Hydrodyn. Ser. B*, vol. 22, no. 6, pp. 856–864, Dec. 2010.

[23] D. Liu and P. Lin, “A numerical study of three-dimensional liquid sloshing in tanks,” *J. Comput. Phys.*, vol. 227, no. 8, pp. 3921–3939, Apr. 2008.

[24] D. Liu and P. Lin, “Three-dimensional liquid sloshing in a tank with baffles,” *Ocean Eng.*, vol. 36, no. 2, pp. 202–212, Feb. 2009.

[25] A. Alemberti *et al.*, “European lead fast reactor—ELSY,” *Nucl. Eng. Des.*, vol. 241, no. 9, pp. 3470–3480, Sep. 2011.

[26] A. Alemberti *et al.*, “ELSY — European LFR Activities,” *J. Nucl. Sci. Technol.*, vol. 48, no. 4, pp. 479–482, 2011.

[27] M. Reale, “Reactor Assembly Configuration Report And Drawings,” ELSY project deliverable DEL/11/020, 2011.

[28] S. Bortot and C. Artioli, “Investigation of the void reactivity effect in large-size Lead Fast Reactors,” *Ann. Nucl. Energy*, vol. 38, no. 5, pp. 1004–1013, 2011.

[29] M. Forni, A. Poggianti, R. Scipinotti, A. Dusi, and E. Manzoni, “Seismic isolation of lead-cooled reactors: The European project SILER,” *Nucl. Eng. Technol.*, vol. 46, no. 5, pp. 595–604, Oct. 2014.

[30] US NRC, “Regulatory Guide 1.60: Design Response Spectra for Seismic Design of Nuclear Power Plants,” *US At. Energy Comm. Washington, DC*, 1973.

[31] G. P. Warn and A. S. Whittaker, “Vertical Earthquake Loads on Seismic Isolation Systems in Bridges,” *J. Struct. Eng.*, vol. 134, no. 11, pp. 1696–1704, Nov. 2008.

[32] G. P. Warn and A. S. Whittaker, “A study of the coupled horizontal-vertical behavior of elastomeric and lead-rubber seismic isolation bearings,” Multidisciplinary Center for Earthquake Engineering Research, 2006.

[33] CD-adapco, “Star-CCM+ v.11.02 User Guide.” 2016.

[34] OECD/NEA Nuclear Science Committee, “Handbook on Lead-bismuth Eutectic Alloy and Lead Properties, Materials Compatibility, Thermal-hydraulics and Technologies,” 2015.

[35] T. Kleefsman, “Water impact loading on offshore structures,” Citeseer, 2005.